Journal of Mechanical Engineering and Automation 2023, 12(1): 1-5
DOI: 10.5923/j.jmea.20231201.01

Numerical and Experimental Studies of a Nonlinear Vibration System

Jasem Alrajhi[1,*], Khalid Alkhulaifi[1], Mohsen Alardhi[1], Khaled Alhaifi[1], Nawaf Alhaifi[1], Ahmed Khalfan[1], Jasem Alazemi[1], Marya Alsaraf[2], Ahmad Khalfan[3]

[1]College of Technological Studies, PAAET, Kuwait
[2]Kuwait Health Ministry, Kuwait
[3]Automotive and Marine Dept., College of Technological Studies, PAAET, Kuwait

Abstract By examining friction pairs surface structural features and using theory of contact mechanics, contact mathematic prototype of microscopic units of thermal distortion friction pairs is made. Using mathematical statistics and normalization method, microscopic model can be removed to macroscopic mathematic model, and then the elastic contact features of friction pairs can be premeditated. A nonlinear dynamic model with five degrees-of-freedom for a four-wheel-drive vehicle driveline coupled by a cardan joint, counting dynamic connection angle, nonconstant velocity, and supplementary instant caused by the cardan joint, is recognized by using the Lagrange method to analyse the driveline coupling vibration in both torsional and lateral directions. High-order Runge–Kutta algorithm is practical to solve the differential equations and to calculate momentary replies of the driveline rotors under acceleration state. The colour maps and second-order vibration of the driveline are attained by frequency spectrum analysis and order tracking analysis, respectively. The second-order vibration and noise of the driveline and vehicle interior caused by the cardan joint is authenticated by vehicle tentative results and condensed efficiently by reducing intersection angle of the cardan joint under the functioning condition. Results shows that application of an elastic coupling as an alternative of the cardan joint knowingly diminishes the second-order vibration but instantaneously creates low-level third-order vibration.

Keywords Nonlinear vibration Numerical Experiment

1. Introduction

In the case of high line speed, the friction pairs of shift clutch of vehicle transmission system will produce thermal distortion in the process of obligatory separation, which will cause vibration and extremely affect the performance of friction element and others related components. The thermal deformation of the friction pairs and its vibration are essential to the design of the clutch of vehicle power-shift steering transmission device. Consequently, it is of significant theoretical and engineering implication to study deeply on the vibration appearances of the friction pairs at high line speed, and to put onward an actual vibration control method to recover the service life of the friction pairs.

By appertain the theory and technology of surface structure features and contact mechanics of friction pairs, from the belvedere of micro mechanics, a microscopic normal element contact model of thermal distortion is recognized. Then making full use of mathematical statistics and standardization methods, the revolution connection between micro and macro is established. Hence, a macro contact mathematical model between two pairs of frictional pairs is obtained. At the same time, with presenting Kelvin-Voigt model and growing the viscoelastic contact differential operator into mathematical model, the viscoelastic contact property including stress and strain is constructed, and a viscoelastic contact mathematical model of the friction pairs can be obtained. At last, the mathematical model of nonlinear vibration is obtained by mechanical analysis, and its vibration characteristics are simulated [1]. The nonlinear vibration characteristics are tested under different rotational speed and lubricating oil, the accuracy of the simulation model is verified.

The passive vibration control of key and subharmonic concurrent resonance for the Duffing-type nonlinear system under the base innervation and external innervation by using magnetorheological (MR) fluid damper is studied, where the fractional-order derivative Bingham model of MR fluid damper is measured [2,3]. The estimated logical solution of the system is attained by using the incremental averaging method.

Based on gaining the principal resonance of the system under base innervation by the averaging method, the

* Corresponding author:
jm.alrajhi@paaet.edu.kw (Jasem Alrajhi)
Received: Feb. 9, 2023; Accepted: Feb. 24, 2023; Published: Mar. 2, 2023
Published online at http://journal.sapub.org/jmea

subharmonic resonance solution of the system is obtained by taking the subharmonic resonance of the system under base innervation and external innervation as an increase so as to obtain the estimated analytical solution of the concurrent resonance of primary and subharmonic resonance [4,5,6]. And the amplitude–frequency equation and phase–frequency equation of the steady-state solutions for the primary and subharmonic resonance of the system are derived respectively. According to the approximate analytical solutions, the steadiness conditions of the steady-state solution of the primary resonance and subharmonic instantaneous resonance are obtained by Lyapunov method.

2. Literature Survey

Al-Mosawe et al. [1], studied the large amplitude nonlinear vibration behaviours of an initially stressed cross-ply composite laminated plate and indicated that the nonlinear dynamic responses are sensitive to the vibration amplitude, aspect ratio, thickness ratio, modulus ratio, stack sequence, layer number, and state of initial stresses. Borowski et al. [2], analysed the nonlinear free vibrations of composite laminated thin plates. Caruntu et al. [3], investigated the nonlinear dynamic behaviours and the chaotic motions of a parametrically excited simply supported rectangular symmetric cross-ply laminated composite thin plate. Krack et al. [4], studied the nonlinear dynamics of a parametrically excited simply supported laminated composite plate and found that there exist the multiple steady bifurcation solutions and jumping under the certain conditions. Lu et al. [5], investigated the bifurcations and chaotic dynamics of a composite laminated piezoelectric rectangular plate with one-to-two internal resonance. Vakakis et al. [6], developed an analytical approximation to solve large amplitude nonlinear free vibrations of a simply supported laminated cross-ply composite thin plate. Kluger et al. [7], studied the nonlinear dynamics and chaotic motions of an angle-ply composite laminated thin plate using third-order shear deformation plate theory. Krack et al. [8], analysed the influence of the quadratic and cubic terms on the nonlinear dynamic characteristics of an angle-ply composite laminated rectangular plate under combined parametric and external excitations. Lu et al. [9], analysed the nonlinear dynamics of a simply supported FGM plate subjected to the transverse and in-plane excitations in a thermal environment. Nayfeh et al. [10], studied the chaotic vibrations of an orthotropic FGM rectangular plate by considering the heat conduction and temperature-dependent material properties. Vakakis et al. [11], investigated the nonlinear oscillations of a cantilever FGM plate based on the third-order deformation plate theory and the asymptotic perturbation method. The various reserchers analysed the nonlinear dynamic responses of a clamped-clamped FGM circular cylindrical shell subjected to an external excitation and uniform temperature change [12,13,14,15].

Using asymptotic perturbation method based on the Fourier expansion and the temporal rescaling, Zewen et al., Yingbing et al. [16,17], investigated the nonlinear oscillations and chaotic dynamics of a simply supported FGM plate.

3. Mathematical Model of Nonlinear Vibration in Sliding Process

1. Dynamic model

A wet clutch friction pair of vehicle transmission system is composed of alternating contact the friction disk and the toroidal dual steel plate. The vibration model of friction pairs of clutches may be divided into several sub vibration models, which means the model is made up of several sub vibration models in series as shown in Figure 1. Each sub vibration model is related to each other by the moment "M" and the axial force "F_n" and each sub model contains only one pair of friction pairs. Based on dynamics and contact mechanics, sub dynamic model can be shown. There, function "F_{nc}" between two contact faces is normal contact force which is made up of scalar sum of elastic contact force and viscoelastic contact force, and function "F_{kn}" is structural stiffness elastic force, and "F_c" is damping force.

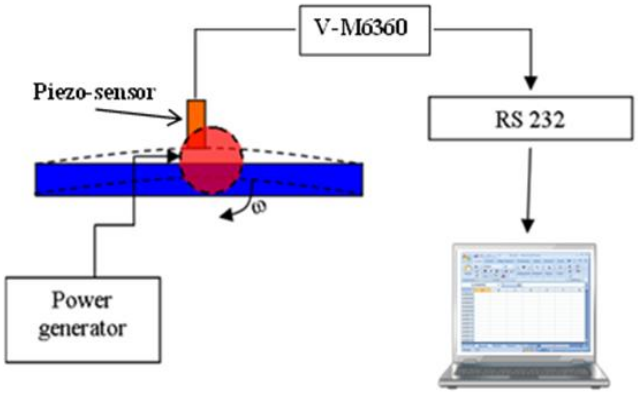

Figure 1. System schematic diagram

According to the actual working conditions of experiment, the initial boundary condition of model is set to include an annular dual steel plate with initial static state and a friction disk with a fixed angular velocity. For making the results to be comparable between simulation and experiment, that is to ensure the consistency of boundary conditions of simulation and test, we suppose that a dual steel plate that would be pressed by the axial force in the friction sliding process, would not be able to rotate around the central line, only to be vibration in the normal direction of the micro displacement. Whereas, in process of sliding, the friction disk not only can rotate, but also the micro displacement vibration of rotating disk can be carried out along the axis direction in the compression process. On condition of axial pressure, when friction pairs are completely combined, the friction disk of model will be fixed in the normal position and cannot rotate around the central line.

The dynamics equation of model is:

$$m_1 x = F_{nc} - F_n \quad (1)$$

$$m_2 x = F_p\ K_n x\ C_n x\ F_{nc} \quad (2)$$

Where F_p is the preload normal force and:

$$F_{kn} = F_p - K_n x \quad (3)$$

Where $F_c = C_n x$ and "x" is the axial direction. From formula (2) the contact force vector F_{nc} is the key to obtain the exact solution of the equation.

2. Normal contact model of micro bulge

At high line speed, the surfaces of friction pairs which has contacted each other will produce local spots at high temperature and pressure and its structure shows the shape of micro bulge as a result of thermoelastic deformation. Therefore, contact model is shown as the form of thermal deformation micro bulge contact. From the contact region centre to the two surfaces direction along the contact normal, not only two surfaces of contact micro bulges are interactive but also the vector direction of Hertz contact force is non-orthogonal with the direction of surface and its direction is angle to normal. According to the Hertz contact force formula, the contact force of micro bulge is:

$$f=4/3\ E\ \beta\ (r)^{1/2}\ w^{3/2} \quad (4)$$

Where "E" is the mixed elastic modulus, "β(r)" is Mixed curvature radius, "w" is the interference in the contact region along the contact normal from the centre to the surface and "r" is the offset distance of the two contact micro bulges in the tangent direction. Thus, when r is 0, two micro bulges are in interference with each other along the normal line from the centre to the plane. However, when r is not 0, two micro bulges are interference along a diagonal line. When two micro bulges curve are in tangent, r is the maximum. Similar to the equivalent curvature in, the interference occurs at the centre of the contact position approximately on the middle of the cross of the undeformed micro bulge.

4. Methods

As the sensor was attached directly at a point on the steel bar to be assumed as the maximum displacement point, the acceleration measurements have been sensed in voltage output. The voltage signal acquired by the sensor was primarily converted by RS 232 from analogue to digital before stored in local PC hard drive and displayed on the PC monitor in real time through the vibrometer software. As the entire test rig components were constructively built, the angular speed of the unbalanced mass should be calibrated. Non-contact tachometer modelled DT-2236 was used to measure the angular speeds of the unbalanced mass when the voltages were varied. To gain the response of the system in frequency domain, the following steps have been done:

1) The voltage of the DC supplier was calibrated with the tachometer to find the relation between the voltage and excitation frequency. In other word, when, the voltage of the DC motor was changed by the DC supplier each time, the frequency of the rotating disc was measured by tachometer.
2) The frequency of excitation has been changed gradually to find the natural frequency of the system. In the natural frequency of the beam, it has been expected to receive maximum amplitude.
3) Around the natural frequency of the system, several runs have been done to find the time response of the system at each frequency of excitation.
4) Maximum amplitude of the vibration has been selected from the time domain at specific excitation frequency.
5) The maximum amplitude at time domain has been drowned verses the related excitation frequency to have the response of the system in frequency domain.

The results of experimental and numerical analysis have been compared for a linear system and a system with nonlinear spring. In the following, the experimental results have been depicted.

5. Result

Table 1. Acquired data of frequency and amplitudes in vibration with non-linearity

RPS	Mm
51.00	0.1922
84.36	0.2670
87.40	1.1129
89.49	1.8356
90.33	2.5248
90.80	2.7898
92.42	3.4303
93.10	4.1303
94.87	4.3222
95.67	4.9280
96.29	5.0473
96.82	5.4836
97.44	5.7291

RPS	mm
102.99	7.9756
103.10	8.0624
103.41	8.2760
103.62	8.5405
104.14	8.6117
104.67	8.7632
105.19	8.7845
106.24	8.9136
109.00	3.9798
113.00	3.1875
114.40	2.8236
120.01	2.3481
121.32	2.3397

RPS	Mm
147.37	1.7720
147.89	1.6130
148.73	1.5460
151.45	1.5300
153.00	1.5120
154.00	1.5000
156.00	1.4400
158.00	1.4980
161.00	1.4300
163.00	1.4440
166.42	1.4100
167.47	1.4263
169.56	1.4469

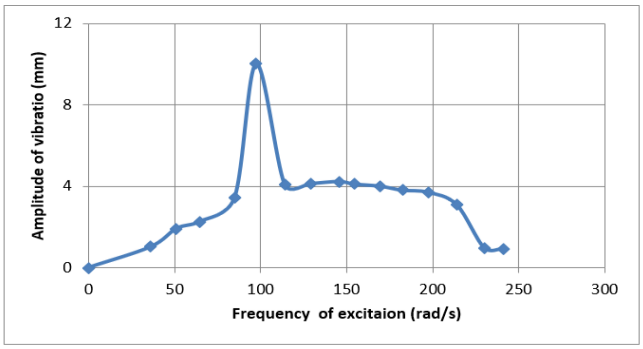

Figure 2. Amplitude of a system without Mag-spring (as the source of nonlinearity) against the excitation frequency of the system

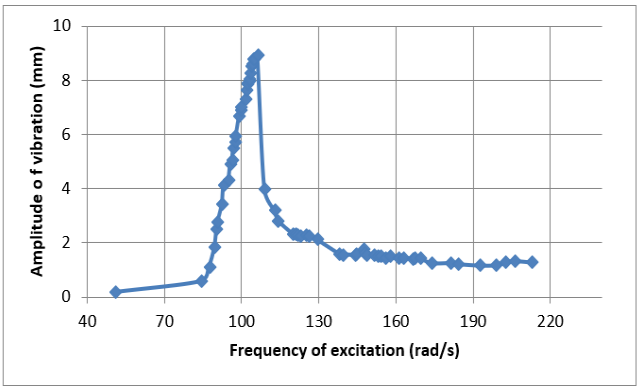

Figure 3. Amplitude of a system with Mag-spring (as the source of nonlinearity) against the excitation frequency of the system

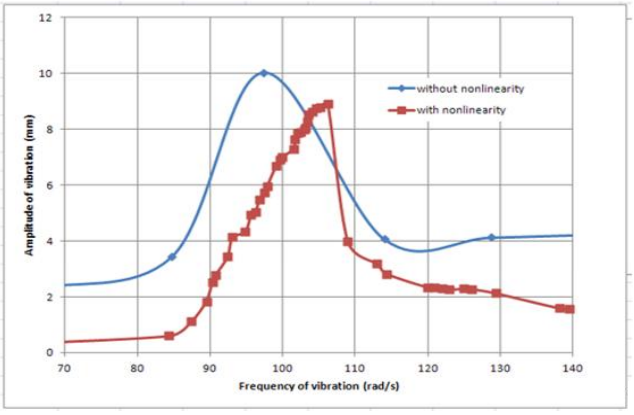

Figure 4. A comparison between two systems with and without nonlinearity (Mag-spring)

6. Discussion

The first part of the study showed how adding Mag-spring as nonlinear stiffness with a hardening behaviour to a single degree of freedom system could protect the system from unwanted vibration at its natural frequency. When the magnitude of the vibration in the system increases because of resonance, automatically the system updates itself and the stiffness of the system will increase as well. The Increase in stiffness will change the natural frequency of the system and as a result it shifts the resonance to a higher frequency. This method leaves the primary system at its designed stiffness, while the system working normally out of resonance range and the stiffness only increases where it is necessary to avoid resonance. Also, the results were compared with the system without any absorber and with a linear absorber. Moreover, the effect of amplitude of the excitation force, F_0, has been studied on the system. In addition, it has been shown how the mass ratio (mass of the absorber over mass of the main system) could modify the natural frequency of the system with two degrees of freedom.

7. Conclusions

A nonlinear dynamic model with five degrees-of-freedom for a four-wheel-drive vehicle driveline has been studied. A nonlinear hardening spring was added numerically and experimentally in parallel to a single degree of freedom (SDOF) system. Results showed that nonlinearity could enhance the behaviour of a system at its primary natural frequency while it is not disturbing the system's stiffness in normal working range (SDOF self-regulating system). Results also showed that nonlinearity could shift the resonance frequency of the SDOF system by 10% (hardening of the system), without affecting the stiffness of the system at normal working condition. The nonlinear absorber could reduce the amplitude of vibration of the main system better than the linear absorber. Moreover, the cancellation range (ω_{n1}-ω_{n2}) was wider about 5% to 10% depending on the system parameters. Damping ratio is important in this kind of design as could seriously affect the cancellation amplitude which is directly used at design of nonlinear absorber. Also, there is an important issue while designing a nonlinear absorber that the amplitude of the absorber should remain limited to the defined area of the nonlinearity.

REFERENCES

[1] Al-Mosawe A, Kalfat R and Al-Mahaidi R. Strength of Cfrp-steel double strap joints under impact loads using genetic programming. Compos Struct 2017; 160: 1205–1211.

[2] Borowski, V.J., Denman, H.H., Cronin, D.L., Shaw, S.W., Hanisko, J.P., Brooks, L.T., Mikulec, D.A., Crum, W.B., Anderson, M.P.: Reducing vibration of reciprocating engines with crankshaft pendulum vibration absorbers. SAE Trans. 100(2), 376–382 (1991).

[3] Caruntu, D.I.: Dynamic modal characteristics of transverse vibrations of cantilevers of parabolic thickness. Mech. Res. Commun. 36(3), 391–404 (2009).

[4] Krack, M., Gross, J.: Harmonic Balance for Nonlinear Vibration Problems. Springer Nature Switzerland, Cham (2019).

[5] Lu, Z., Wang, Z., Zhou, Y., Lu, X.: Nonlinear dissipative devices in structural vibration control: a review. J. Sound Vib. 423 (June 9), 18–49 (2018).

[6] Vakakis, A.F., Gendelman, O., Bergman, L.A., McFarland, D.M., Kerschen, G., Lee, Y.S.: Nonlinear Targeted Energy Transfer in Mechanical and Structural Systems. Springer, Berlin (2008).

[7] Kluger, J.M., Sapsis, T.P., Slocum, A.H.: Robust energy harvesting from walking vibrations by means of nonlinear cantilever beams. J. Sound Vib. 341 (April 14), 174–194 (2015).

[8] Krack, M., Gross, J.: Harmonic Balance for Nonlinear Vibration Problems. Springer Nature Switzerland, Cham (2019).

[9] Lu, Z., Wang, Z., Zhou, Y., Lu, X.: Nonlinear dissipative devices in structural vibration control: a review. J. Sound Vib. 423(June 9), 18–49 (2018).

[10] Nayfeh, A.H., Balachandran, B.: Applied Nonlinear Dynamics, 2nd edn. Wiley-VCH, Weinheim (2004).

[11] Vakakis, A.F., Gendelman, O., Bergman, L.A., McFarland, D.M., Kerschen, G., Lee, Y.S.: Nonlinear Targeted Energy Transfer in Mechanical and Structural Systems. Springer, Berlin (2008).

[12] Wang, J., Wierschem, N., Spencer, B.F., Lu, X.: Experimental study of track nonlinear energy sinks for dynamic response reduction. Eng. Struct. 94 (July 1), 9–15 (2015).

[13] Yuan, Z., Liu, W., Zhang, S., Zhu, Q., Hu, G.: Bandwidth broadening through stiffness merging using the nonlinear cantilever generator. Mech. Syst. Signal Process. 132, 1–17 (2019).

[14] P.L. Grossman, B. Koplik, Y.Y. Yu, Nonlinear vibrations of shallow spherical shells. J. Appl. Mech. 36(3), 451–458 (1969).

[15] M. Strozzi, F. Pellicano, Nonlinear vibrations of functionally graded cylindrical shells. Thin-Walled Struct. 67, 63–77 (2013).

[16] Zewen Gu, Xiaonan Hou and Jianqiao Ye, Design and analysis method of nonlinear helical springs using a combining technique: Finite element analysis, constrained Latin hypercube sampling and genetic programming Proc IMechE Part C: J Mechanical Engineering Science IMechE 2021 Vol 235(22) 5917-5930.

[17] Yingbing Su 1, Huaiwu Zou 2, Hongrun Lu 3, Bingshan Hu 1,4,* and Hongliu Yu 1,4 Design and Control of a Nonlinear Series Elastic Cable Actuator Based on the Hill Muscle Model Actuators 2022, 11, 68. https://doi.org/10.3390/act11030068.